International Journal of
Emerging Research in Management &Technology
ISSN: 2278-9359 (Volume-5, Issue-8)

Research Article | **August 2016**

Thermohaline Convection with Variable Viscosity in a Porous Media

S. Hari Singh Naik
Department of Mathematics University College of Science Osmania University,
Hyderabad, Telangana, India

Abstract:

The problem of double diffusive convection with variable viscosity confined between the two horizontal plates is investigated by the linear stability analysis. The transformed governing equations are numerically solved by using the Galerkin method. We have studied both stationary convection and oscillatory convection. The threshold values of Rayleigh number and wave number are computed and presented for various boundary conditions viz. rigid-rigid (R/R), ***rigid-free*** (R/F), ***free-rigid*** (F/R) ***and free-free*** (F/F) ***and for different values of physical parameters viz., salinity Rayleigh number*** R_s, ***Lewis number L, viscosity ratio c and Prandtl number*** P_r. ***For rigid-rigid boundary conditions we have studied the effect of*** c, R_s ***on the vertical velocity and temperature eigenfunctions at the onset. It is observed that the salinity concentration stabilizes the dynamical system. The occurrence of co-dimension two bifurcation point*** (CTP) ***is shown for various boundary conditions.***

Keywords: Thermohaline convection, Variable viscosity, Exponential fluid, Galerkin method.

I. INTRODUCTION

The study of flow through porous media continues to receive considerable attention due to its many practical applications in the physical, biological and applied sciences. On the one hand, the movement of ground water is represented by flow through porous media, the study of which is essential in the recovery of fresh water [1], [2]. In addition, the increasing demand for energy necessitates the study of oil and gas movement through the porous earth layers. Interaction of oil, gas and water, their movement and the displacement processes that occur within the oil reservoir is a study of fundamental importance in this field [3], [4].In agriculture, the importance of flow through porous media is witnessed in irrigation processes and the movement of nutrients, fertilizers and pollutants in to plants [5], [6]. The study of convection processes in porous media has also received considerable attention in the literature due to the importance of these processes in geothermal, geophysical and industrial environment, where analysis of thermal energy storage systems, thermal insulation and solar collectors with porous absorbers is vital [7], [8]. A large portion of the literature on flow through porous media reports on heat and mass transfer in composite material, which finds applications ranging from environmental and geothermal to energy storage systems. Advances in this field are reported in the pioneering works of Rudraiah, Neild, Bejan and Kaviani among others ([8], [9], [10], [11]).

Further application of flow through porous media are exhibited in the biological sciences and in biomechanics where, for example, the human lungs and tissues are idealized into layers of floes and other types of porous materials [12]. Applications of flow through porous media in the study of biological and macromolecular systems have been reported by various authors [13], [14], [15]. Moreover, studies on diffusion controlled processes in porous media, which finds applications in many areas including the drying of solids [16].

The flow of various fluids are described mathematically by a set of equations representing two conservation principles, conservation of mass and conservation of momentum. When a fluid is Newtonian, the momentum equations are given by the Navier-Stokes equations, which, when the fluid is incompressible and the body forces are neglected. Depending on the type of the porous medium and the flow under consideration, the macroscopic momentum equations may be classified as Darcian and non-Darcian models. The macroscopic forms and the ranges of validity of some of the leading models are discussed in the following sections.

In 1856, Darcy conducted an experiment that resulted in what is now known as Darcy's law, which has been generalized for three-dimensional flow and cast in the differential form by Muskat [4].

Darcy's law is postulated to have some limitations on its validity [17], [18], [19]. The most important limitations are when the flow is of the seepage type and the fluid is homogeneous. Thus, Darcy's law can be considered to be valid in situations where the flow is of the creeping type [5] or when the porous medium is densely packed with small enough permeability (K)([20], [6]) $\sqrt{K} < 1$, such that the pore Reynolds number based on the local volume averaged speed, is less than unity.

Darcy's law neglects the boundary and inertial effects of the fluid flow due to the small porosity associated with the medium. In certain types of porous Medias,where the porosity is close to unity and the flow is of high enough speed such that the pore Reynolds number is of order unity or greater, the inertial effects, which arise due to the curvilinearity of the flow path, have to be taken into account. Furthermore, the Darcy's law does not account for the high velocity gradients that arise when the viscous effects are important, especially in the presence of a solid wall, due to the low order of this law. At this point, one must reject Darcy's law and employ a non-Darcy

©2016, IJERMT All Rights Reserved

equation that incorporates inertial and / or viscous shear effects.

Although Darcy-Lpwood and Darcy-Forchheimer models take into account the fluid inertia, they neglect the viscous shearing action. It might be argued that the Laplacian of the velocity is small in the porous medium, and thus the flow behaves Darcy like in the core of the porous medium. However, the presence of a solid wall, near the velocity gradient is high, necessitates taking into account the viscous shearing action. The Laplacian of the velocity thus becomes significant, but a proper definition of porosity near the solid boundary in this case is essential [21].

The scheme of paper is the following one. In Section 2 we obtain the non-dimensional perturbation equations of the thermohaline convection for exponential fluids. In section 3 we have studied the linear stability analysis. Numerical results are presented in Section 4. Finally, conclusions are made in Section 5.

II. MATHEMATICAL FORMULATION

A quiescent layer of a two-component fluid, saturating with a porous medium, is confined between the boundaries at $z = -d/2$and $z = d/2$.In the Boussinesq approximation the governing equations for the thermohaline convection with variable viscosity in a sparsely packed porous media (See Fig. 5.1) in dimensional form are given by:

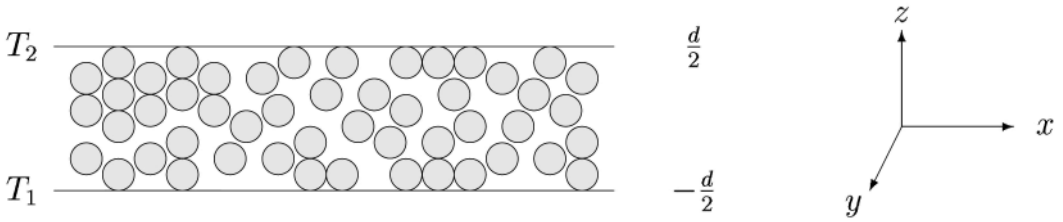

Figure 1: Schematic diagram of sparsely packed porous media, where upper and lower boundaries located at $z = d/2$and $z = -d/2$,respectively.

the equation of continuity

$$\nabla'.\vec{V}' = 0, \qquad (1)$$

the momentum equation

$$\rho_0\left(\frac{1}{\phi}\frac{\partial}{\partial t} + \frac{1}{\phi^2}\vec{V}'.\nabla'\right)\vec{V}' = -\nabla'P' + \rho_0\left(K_1\hat{\imath} + K_2\hat{\jmath} + K_3\hat{k}\right) + \rho\vec{g} - \frac{\mu}{K}\vec{V}', \quad (2)$$

the heat equation

$$M\frac{\partial T'}{\partial t'} + \left(\nabla'.\vec{V}'\right)T' = K\nabla'^2T' + v\Phi, \quad (3)$$

and the concentration equation

$$\frac{\partial S'}{\partial t'} + \left(\vec{V}'.\nabla'\right)S' = K_s\nabla'^2S', \quad (4)$$

where in eq. (5.2.2)

$$K_1 = 2\mu\frac{\partial^2 u'}{\partial x'^2} + \frac{\partial}{\partial y'}\left[\mu\left(\frac{\partial u'}{\partial y'} + \frac{\partial u'}{\partial x'}\right)\right] + \frac{\partial}{\partial z'}\left[\mu\left(\frac{\partial w'}{\partial x'} + \frac{\partial u'}{\partial z'}\right)\right],$$

$$K_2 = 2\mu\frac{\partial^2 v'}{\partial y'^2} + \frac{\partial}{\partial z'}\left[\mu\left(\frac{\partial v'}{\partial z'} + \frac{\partial w'}{\partial y'}\right)\right] + \frac{\partial}{\partial x'}\left[\mu\left(\frac{\partial u'}{\partial y'} + \frac{\partial v'}{\partial x'}\right)\right],$$

$$K_3 = \frac{\partial}{\partial z'}\left[2\mu\frac{\partial w'}{\partial z'}\right] + \frac{\partial}{\partial x'}\left[\mu\left(\frac{\partial w'}{\partial x'} + \frac{\partial u'}{\partial z'}\right)\right] + \frac{\partial}{\partial y'}\left[\mu\left(\frac{\partial u'}{\partial z'} + \frac{\partial u'}{\partial y'}\right)\right].$$

$$\Phi = 2\left[\left(\frac{\partial u}{\partial x}\right)^2 + \left(\frac{\partial u}{\partial y}\right)^2 + \left(\frac{\partial w}{\partial z}\right)^2 + \left(\frac{\partial v}{\partial x} + \frac{\partial u}{\partial x}\right)^2 + \left(\frac{\partial w}{\partial y} + \frac{\partial v}{\partial z}\right)^2 + \left(\frac{\partial u}{\partial z} + \frac{\partial w}{\partial x}\right)^2 - \frac{2}{3}\left(\left(\frac{\partial u}{\partial x} + \frac{\partial v}{\partial y} + \frac{\partial w}{\partial z}\right)^2\right)\right],$$

where$\vec{V}'(u', v', w')$is the mean filter velocity of the fluid, $P'$is the pressure, $M = \frac{(\rho^C)m}{(\rho^C p)_f}$is thedimensionless heat capacity and K is the permeability of the porous medium. Since our interest here is a liquid saturated porous medium, the heat capacity ratio, M, can be assumed, with sufficient accuracy to be unity (i.e., M = 1) (Rudraiah et al. [26]).

When a salt is added to a volume of water the volume increases, an effect that tends to decrease the density, but the total density of the fluid increases. Let $\beta_s$measures this density increase. Thus in thermohaline convection density variations depends on both diffusive mechanisms. Thus the variation may be taken as([22], [23], [24], [25], [26]):

$$\rho = \rho_0\left[1 - \alpha(T' - T_1') + \beta_s\left(S' - S_b'\right)\right], \qquad (5)$$

$$\rho = \rho_0\left[1 - \alpha(T' - T_1') + \beta_s\left(S' - S_b'\right)\right], \qquad (6)$$

with

$$\alpha = -\frac{1}{\rho_0}\left(\frac{\partial\rho}{\partial T'}\right)\text{and}\beta_s = -\frac{1}{\rho_0}\left(\frac{\partial\rho}{\partial S'}\right).$$

here$\rho_0$is the mean density of the system, T' and S' temperature and salinity concentration of the system, respectively, $\alpha$is thermal expansion coefficient and$\beta_s$is the coefficient of density increase with respect to salinity.

The choice of the density variation will depend upon the physics of the double diffusive system. If the heavier

©2016, IJERMT All Rights Reserved

component of the fluid is introduced in the system, then due to the diffusion of mass there results an increase in the density of the mixture in which case the relation (5) is suitable. If the lighter component is introduced then the mass diffusion lowers the density of the mixture, hence the validity of relation (6).
The solutions at the static state are given by

$$\vec{V}' = 0,$$
$$T_s' = T_1' - (\Delta T'/d)z', S_s' = S_b' - (\Delta S'/d)z',$$
$$P_s' = P_0' + z'\vec{g} + \alpha\beta\vec{g}\frac{z'^2}{2}.$$

The convection state is characterized by introducing small perturbations in the static state solutions given by
$\vec{V}' = \vec{V}'s + \vec{V}'^*, T' = T_s' + \theta'^*,\ P' = P_s' + P'^*,\ C' = S' + S_s'^*$.(7)
We non-dimensionalize the eqs. (1)-(4) by using the following scaling

$$x = \frac{x'}{d}, y = \frac{y'}{d}, z = \frac{z'}{d}, u = \frac{u'}{kd^{-1}},, v = \frac{v'}{kd^{-1}},, w = \frac{w'}{kd^{-1}},$$
$$\theta = \frac{\theta'}{\Delta T'}, p = \frac{p'}{\rho' k^2 d^{-2}}, C = C'/\Delta S', \qquad (8)$$

The basic dimensionless perturbed equations in the Boussinesq approximation can be written as:

$$\nabla.\vec{V} = 0, \qquad (9)$$
$$\frac{1}{P_r}\left[\frac{1}{\phi}\frac{\partial\vec{V}}{\partial t} + \frac{1}{\phi^2}(\nabla.\vec{V})\vec{V}\right] = -\frac{\nabla P_1}{P_r} + (R_T\theta - R_sC)\hat{e}_z +$$
$$\hat{e}_z\left[2f\frac{\partial^2 u}{\partial_{x^2}} + \frac{\partial}{\partial z}\left(f\left(\frac{\partial w}{\partial x} + \frac{\partial u}{\partial z}\right)\right)\right] + \hat{e}_y\left[\frac{\partial}{\partial z}\left(f\frac{\partial v}{\partial z}\right) + \frac{\partial}{\partial x}\left(f\frac{\partial v}{\partial x}\right)\right] +$$
$$+\hat{e}_z\left[\frac{\partial}{\partial z}\left(2f\frac{\partial w}{\partial z}\right) + \frac{\partial}{\partial z}\left(f\left(\frac{\partial w}{\partial x} + \frac{\partial u}{\partial z}\right)\right)\right] - \frac{1}{D_a}f\vec{V}, \qquad (10)$$
$$\left[\frac{\partial}{\partial t} + (\vec{V}.\nabla)\right]\theta = w + \nabla^2\theta, \qquad (11)$$
$$\frac{1}{L}\left[\frac{\partial C}{\partial t} + (\vec{V}.\nabla)C\right] = \frac{w}{L} + \nabla^2 C. \qquad (12)$$

The z-component of the curl of curl of the momentum equation (10) is given by

$$\left(\frac{1}{P_r\phi}\frac{\partial}{\partial t} - f\nabla^2\right)\nabla^2 w - 2\frac{df}{\partial z}\nabla^2\frac{\partial w}{\partial z} + \frac{d^2 f}{\nabla z^2}\left(\frac{\partial^2}{dx^2} + \frac{\partial^2}{dz^2}\right)w + (R_T\theta - R_sC)\nabla_h^2 w +$$
$$\frac{1}{D_a}\left[f\left(\frac{\partial^2}{dx^2} + \frac{\partial^2}{dz^2}\right)w - \frac{df}{\partial z}\frac{\partial w}{\partial z}\right] = \hat{e}_z.\frac{1}{P_r}\left[\nabla\times\nabla\times(\vec{V}.\nabla)\vec{V}\right]. \qquad (13)$$

The variable viscosity $v(z) = u/\rho_0$ is given by $v(z) = v_0 f(z)$, where v_0 is the reference value of the kinematic viscosity evaluated at T_0 and $f(= v/v_0)$ is the dimensionless viscosity ratio.
We have considered the non-dimensional viscosity variations as:
$f = \exp[c(T_0 - T)]$, (14)
where

$$c = \log\left(\frac{v_{max}}{v_{min}}\right) = \log\left(\frac{1+\gamma}{1-\gamma}\right), 0 \le \gamma < 1.$$

III. LINEAR STABILITY ANALYSIS

In this section, we study the linear stability of the static solution. To examine the stability of the linearized equations of (11)-(13), we take the normal mode solutions of the form
$[w, \theta, C] = [W(z),\ \Theta(z),\ C(z)]\exp(iqx + pt)$, (15)
where $W(z)$, $\Theta(z)$ and $C(z)$ are the eigenfunctions and p denotes the growth rate of the perturbations and q denotes the wave number. Using the above set of solutions (15) into the linear parts of the eqs. (11)-(13), we get

$$\frac{p}{P_r\phi}(D^2 - q^2)W = (D^2 f)(D^2 + q^2)W + (2Df)(D^2 - q^2)^2$$
$$DW + f(D^2 - q^2)^2 W - \frac{1}{D_a}[f(D^2 + q^2)W + DfDW] - R_T q^2\Theta + R_s q^2 C, \qquad (16)$$
$$p\Theta = (D^2 - q^2)\Theta + W, \qquad (17)$$
$$\frac{p}{L}C = (D^2 - q^2)C + \frac{W}{L}. \qquad (18)$$

Here $D = d/dz$ is the differential operator, q is the overall horizontal wave number, W is the z-part of the vertical component of the velocity, Θ is the z-part of temperature, C is the amplitude of concentration. The physical parameters are R_T is the thermal Rayleigh number, R_s is the salinity Rayleigh number, P_r is the Prandtl number, L is the Lewis number, ϕ is the porosity parameter and $D_a = K/d^2$ is the Darcy number, K is the permeability of the medium.

3.1 Boundary Conditions

The linearized eqs. (16)-(18) are analyzed by considering four types of boundary conditions namely, $(R/R), (R/F), (F/R)$, and (F/F).
(i) No slip condition on the top and bottom boundaries (R/R).i.e.,
$W = DW = \Theta = C = 0$ at $z = 1/2, z = -1/2$. (19)
(ii) Stress-free condition at the top $(z = 1/2)$ and no slip condition at the bottom $(z = -1/2)$ boundaries

©2016, IJERMT All Rights Reserved

(F/R).i.e.,

$$W = D^2W = \Theta = C = 0 \quad \text{at} \quad z = 1/2,$$
$$W = DW = \Theta = C = 0 \quad \text{at} \quad z = -1/2, \quad (20)$$

(iii) No slip condition at the top $(z = 1/2)$ and stress free condition at the bottom $(z = -1/2)$ boundaries(R/F). i.e.,

$$W = DW = \Theta = C = 0 \text{at} z = 1/2,$$
$$W = D^2W = \Theta = C = 0 \text{at} z = -1/2, \quad (21)$$

(iv) Stress-free condition at the top and bottom boundaries(F/F).i.e.,

$$W = D^2W = \Theta = C = 0 \text{at} z = 1/2, z = -1/2 (22)$$

where$D = d/dz$.

The Galerkin method is one technique of obtaining approximate solutions of the differential equations. It involves the expansion of the solution in a series of trial functions with unknown coefficients. The coefficients are determined such that the series is a good approximation to the solution of the differential equations.

The Galerkin method is much like a Fourier series expansion except that the trial functions are not necessarily orthogonal and, instead of seeking periodic solutions, the trial functions are chosen so that they satisfy the boundary conditions.

The unknown variables $W(z)$,$C(z)$ and $\Theta(z)$are expanded in terms of the following complete sets of trial functions, that satisfy the homogeneous boundary conditions (19)-(22)

$W(z) = \sum_{n=1}^{\infty} a_n W_n(z), \quad C(z) = \sum_{n=1}^{\infty} b_n C_n(z)$and $\Theta(z) = \sum_{n=1}^{\infty} c_n \Theta_n(z)$,(23)

where $W_n(z)$, $C_n(z)$and $\Theta_n(z)$are the trial functions that satisfy the homogeneous boundary conditions (19)-(22), and the coefficients and a_n, $b_n$and $c_n$are unknown constants. The trial functions that satisfy the no-slip boundary conditions (5.3.5) are chosen as:

$$W_n(z) = \begin{cases} \frac{\cosh(\alpha_n z)}{\cosh\left(\frac{\alpha_n}{2}\right)} - \frac{\cos(\alpha_n z)}{\cos\left(\frac{\alpha_n}{2}\right)}, & n \text{ is odd} \\ \frac{\sinh(\alpha_n z)}{\sinh(\alpha_n/2)} - \frac{\sin(\alpha_n z)}{\sin(\alpha_n/2)}, & n \text{ is even} \end{cases} \quad (24)$$

where the constants $a_n$are zeros of

$$\tanh(\alpha_n/2) + \tan(\alpha_n/2) = 0, \ n \text{ is odd}$$
$$\coth(\alpha_n/2) + \cot(\alpha_n/2) = 0, \ n \text{ is even}$$

The function $C_n(z)$ is given by

$$C_n(z) = \begin{cases} \cos(n\pi z), & n \text{ is odd} \\ \sin(n\pi z), & n \text{ is even} \end{cases} \quad (25)$$

The function $\Theta_n(z)$ is given by

$$\Theta_n(z) = \begin{cases} \cos(n\pi z), & n \text{ is odd} \\ \sin(n\pi z), & n \text{ is even} \end{cases} \quad (26)$$

Similarly, we can choose the trial functions for the remaining boundary conditions viz.,R/F, F/R, F/F.

The trial functions with unknown coefficients are substituted into the differential equation (16)-(18). In general, the equation will not be satisfied, there will exist a residual which the Galerkinmethod seek to minimize. The unknown coefficients are determined by requiring that the residuals be orthogonal to each of the trial functions. We get the matrix eigenvalue problem

$$(U - pV)X = 0, \ (27)$$

where*U*, *V* and *X* are the matrices and they are given by

$$U = \begin{pmatrix} B_{ji} & C_{ji} & D_{ji} \\ F_{ji} & G_{ji} & H_{ji} \\ J_{ji} & K_{ji} & L_{ji} \end{pmatrix}, \ V = \begin{pmatrix} A_{ji} & 0 & 0 \\ 0 & E_{ji} & 0 \\ 0 & 0 & I_{ji} \end{pmatrix}, \ X = \begin{pmatrix} a_n \\ b_n \\ c_n \end{pmatrix}. (28)$$

The matrix elements in eq. (28) are defined as

$$A_{ji} = \frac{1}{P_r \phi} \langle W_j D^2 W_i - q^2 W_j W_i \rangle,$$
$$B_{ji} = \langle (D^2 f)\left(W_j D^2 W_i + q^2 W_j W_i\right) + (2Df)\left(W_j D^3 W_i + q^2 W_j W_i\right)$$
$$+ f\left(W_j D^4 W_i - 2q^2 W_j D^2 W_i + q^4 W_j W_i\right) - \frac{1}{D_a}[f(D^2 + q^2)W + DfDW] \rangle$$
$$C_{ji} = -R_T q^2 \langle W_j \Theta_i \rangle, \ D_{ji} = -R_s q^2 \langle W_j C_i \rangle, \quad E_{ji} = \langle \Theta_j \Theta_i \rangle,$$
$$F_{ji} = \langle \Theta_j W_i \rangle, \ D_{ji} = \langle \Theta_j D^2 \Theta_i - q^2 \Theta_j \Theta_i \rangle,$$
$$H_{ji} = \langle 0 \rangle, \ I_{ji} = \frac{1}{L} \langle C_j C_i \rangle, \quad J_{ji} = \frac{1}{L} \langle C_j W_i \rangle,$$
$$K_{ji} = \langle 0 \rangle, \ L_{ji} = \langle C_j D^2 C_i - q^2 C_j C_i \rangle, \quad (29)$$

©2016, IJERMT All Rights Reserved

and the angular bracket expression represents

$$\langle h_1(z)h_2(z)\rangle = \int_{-1/2}^{1/2} h_1(z)h_2(z)dz,$$

where $h_1(z)$ and $h_2(z)$ are the orthogonal functions. For the non-trivial solutions, the system of eqs. (27) gives the characteristic equation as:

$$|U - pV| = 0.(30)$$

The system of eqs. (27) is solved as a generalized eigenvalue problem. This task is accomplished numerically, by making this infinite set of equations to finite by the numerical truncation. The real parts of the eigenvalues, say, $Re(p_k) < 0$ determine the stability of the system. If $Re(p_k) < 0$ for all k, the system is said to be stable. If $Re(p_k) > 0$ for at least one value of k, the system is unstable. The marginal stability curve corresponds to the case when one of the eigenvalues satisfies $Re(p_k) = 0$.The eigenvalue p is a function of the physical parameters R_T, q, $R_s c$, P_r, L, D_a and $f(z)$.The parameter R_T determines the onset of instabilities and depends on the physical parameters q, $R_s c$, P_r, L, D_a and $f(z)$.At each q the number of eigenvalues depends on the trial functions used in eq. (23). Only those R_T values that are real, positive and finite are considered to be physically meaningful. For any q we take the smallest of these meaningful R_T values. We obtain critical value of R_T by iterating q until the marginal stable value of R_T is minimized. The convective system can be unstable to either stationary convection or oscillatory convection at the onset of instability. The occurrence of stationary convection or oscillatory convection in the convective system depends on the physical parameters. The critical Rayleigh number R_{sc} is obtained from $\partial R_s/\partial q = 0$.

3.2 Stationary Convection

The stationary convection is obtained when one of the eigenvalues, p_k vanishes. Thus, the Rayleigh number for the stationary convection, $R_T = R_s$ is obtained from eq. (29) for $i = j = 1$ as:

$$R_s = \frac{I_{11}D_{11}G_{11} + B_{11}H_{11}J_{11} + E_{11}D_{11}J_{11} - B_{11}G_{11}L_{11}}{C(I_{11}H_{11} - E_{11}L_{11})} \quad (31)$$

It can be observed that the matrix elements on the right hand side of the above eq. (31) are independent of P_r.Hence the critical Rayleigh number for stationary convection is independent of P_r.The critical Rayleigh number $R_T = R_{sc}$ and the critical wave number $q = q_{sc}$ for the onset of stationary convection depends on the physical parameters R_s, L, D_a and c.

3.3 Oscillatory Convection

The condition for oscillatory convection are given by $p_k = \pm iw$, where w is the frequency of the oscillations and $w^2 > 0$, where

$$w^2 = \frac{1}{A_{11}F_{11}K_{11}}\Big[B_{11}F_{11}L_{11-} + E_{11}C_{11}K_{11}R_T - I_{11}D_{11}F_{11} + A_{11}G_{11}L_{11} + B_{11}G_{11}K_{11} - A_{11}H_{11}J_{11}\Big].(32)$$

The Rayleigh number for the oscillatory convection $(R_T = R_0)$ is given by:

$$R_0 = \frac{M}{K_{11}C_{11}(I_{11}H_{11}A_{11}F_{11} + E_{11}B_{11}F_{11}K_{11} + E_{11}A_{11}G_{11}K_{11})}, \quad (33)$$

where

$$M = 2B_{11}G_{11}L_{11}A_{11}F_{11}K_{11} + B_{11}^2F_{11}K_{11}^2G_{11} + B_{11}^2F_{11}^2K_{11}L_{11} - B_{11}F_{11}^2K_{11}I_{11}D_{11} + A_{11}G_{11}^2K_{11}^2B_{11} - A_{11}^2G_{11}K_{11}H_{11}J_{11}A_{11}F_{11}^2L_{11}^2B_{11} - A_{11}F_{11}^2L_{11}I_{11}D_{11} + A_{11}^2F_{11}L_{11}^2G_{11} - A_{11}^2F_{11}L_{11}H_{11}J_{11} - E_{11}D_{11}J_{11}A_{11}F_{11}K_{11}.$$

The quantities given in eqs. (31), (32) and (33) are obtained from eq. (29) for $i = j = 1$. The critical Rayleigh number at $R_T = R_{0c}$ and critical wave number at $q = q_{0c}$,for various types of boundary conditions, are computed when $w^2 > 0$. The threshold values of R_{0c} and q_{0c} depends on L, P_r, R_s, D_a and c. The critical Rayleigh number R_{sc} is obtained from $\partial R_0/\partial q = 0$. For the present physical system, Pr is finite. The time dependent convective flow exists when $R_T = R_{oc}$.At $R_T = R_{sc}, q = q_{sc}$ and at $R_T = R_{oc}, q = q_{oc}$ we get the pitchfork bifurcation and the Hopf bifurcation, respectively. The pitchfork and the Hopf bifurcation are known as the primary bifurcations (co-dimension one bifurcation point). Pitchfork bifurcation arises when the characteristic eq. (30) possesses a simple zero eigenvalue. Hopf bifurcation arises when a pair of purely imaginary complex conjugate eigenvalues are obtained from the characteristic eq. (30). The secondary bifurcations, viz., Tokens-Bogdanov bifurcation point $(w^2 = 0)$ and co-dimension two bifurcation point (CTP)$(w^2 > 0)$, occurs on combining Rayleigh numbers and wave numbers of stationary convection and oscillatory convection. At the CTP, we get $R_{sc} = R_{oc}$ but $q_{sc} \neq q_{oc}$.The intersection point of the neutral curves of stationary convection and oscillatory convection in the $(c,\ R_c)$-plane gives CTP and it is discussed in detail in the following section.

IV. RESULTS AND DISCUSSION

The linear stability analysis is carried out with viscosity depending exponentially on temperature at the onset of. The resulting eigenvalue problem is solved numerically by employing the Galerkin technique for various combinations of boundary conditions viz., $R/R, R/F, F/R$, and F/F.The parameters which are influencing the

©2016, IJERMT All Rights Reserved

criterion for the onset of convection are the salinity Rayleigh number R_s,Lewis number L, Prandtl number P_r, Darcy number $D_a$and the viscosity ratio c. The behaviour of these parameters are exhibited in Figures 2 to 15.

In Figures 2 (a-d), we have studied the effect of c on critical Rayleigh number for large (infinite) P_r.Figures 2 (a-d) are plotted for $R/R, R/F, F/R,$ and F/Fboundary conditions respectively. Figure 2(a), shows that as c increases R_{sc}decreases, but this is not consistent with the increasing values of c. This implies that the effect of viscosity variation destabilizes the convective system. We can also observe that the value of R_{sc}at $c = 0$ is more than the value of R_{sc}at $c \neq 0$. This implies that in a double diffusive convection with porous media,the onset of convection for a constant viscosity fluid differs from that of the variable viscosity fluid.

We have also studied the effect of $R_s$on $R_{sc}$for the given set of physical parameters. This Fig. 2(a) shows that as $R_s > 0$,increases R_{sc}increases. This implies that the effect of $R_s$stabilizes the convective system. Figures 2 (b), (c) and (d), show the similar results. We can also observe that the Figs. 2(b) and 2(c) show very close results.

In Figs. 3(a-d), we have studied the effect of c and $R_s$on the $q_{sc}$for $R/R, R/F, F/R,$ and F/Fboundary conditions, respectively, for large (infinite) P_r.Figure 2(a), shows that as c increases q_{sc}increases slowly for small values of c and q_{sc}increases considerably for further increment values of c . This figure also shows that as $R_s$increases q_{sc}also increases. The results of $R/F$and F/Rboundary conditions are close to each other. Figures 3(b) and (c) show that the effect of $R_s$on $q_{sc}$is small for low viscosity variation values of c.

Figures 4(a-d) show the effect of L on $R_{sc}$for a given set of physical parameters. These figures show that, as L increases R_{sc} decreases. This implies that effect of Lewis number destabilizes the convective system. This phenomenon is similar for other boundary conditions. In Figures 5(a-d), we studied the effect of L on $q_{sc}$and observed that as L increases q_{sc}increases for all set of boundary conditions.

Figures 6(a-d), are plotted for finite P_r.Figures 6(a, c) and 6(b, d) are plotted for $R/R$and F/Fboundary conditions, respectively. From Figure 6(a) we can see that oscillatory convection occurs as a first instability. From this figure we can observe that, as c increases R_{0c}deceases. This implies that the effect of c destabilizes the onset of oscillatory convection. From this figure we also observe that, R_{0c}increases with increasing R_s.This implies that the effect of $R_s$stabilizes the onset of oscillatory convection. The effect of c and Rs are shown on q_{0c}in Figs. 6 (c) and (d).

In Figs. 7(a) and 7(b), we have studied the effect of L on $R_c$for R/R and F/Fboundary conditions, respectively. These figures show that oscillatory convection exists at the onset of convection for finite value of P_r.We can see that as L increases R_{0c}decreases. This implies that the effect of L destabilizes the onset of oscillatory convection. The effect of L on $q_{0c}$is shown in Figs. 7(a) and (d) for R/R and F/F boundary conditions, respectively. From these figures we can observe that, as c increases q_{0c}increases. The effect of $P_r$is shown in Figures 8(a) and (b) at the onset of convection for R/R and F/Fboundary conditions, respectively. From these figures we can observe that oscillatory convection occurs as a first instability at the onset. Figs. 8(a) and (b) show that as $P_r$increasesR_{0c} decreases. This implies that the effect of $P_r$destabilizes the over stability. The effect of $P_r$on $q_{0c}$is shown in Figs. 7(c) and (d), for R/R and F/Fboundary conditions, respectively. From these figures we can observe that as $P_r$increases, q_{0c}increases.

Figures 9 (a-c) show the effect of physical parameters R_s,L,P_r, Daon $w^2$for R/Rboundary conditions. Until a moderate viscosity ratio, c, frequency $w^2$is almost constant. For large viscosity variation, w^2increases. The frequencyw^2, decreases as $R_s$and L increases, while the opposite trend is observed with respect to Pr. Figure 10 shows the vertical velocity eigenfunctions $W(z)$as a function of the depth, L, $D_a$and $R_s$with R/Rboundary conditions for several values of viscosity ratio c.From this figure, we can observe that for $c = 0$the velocity is symmetric about the midpoint of the layer. As the ratio of viscosity, to the top and bottom boundaries, increases the maximum velocity of the fluid particles is near the bottom of the fluid layer where the fluid is less viscous. Figure 11, shows the variation of temperature eigenfunction $\Theta(z)$as a function of depth z, c and $R_s$with R/Rboundary conditions. From this figure we can observe that $\Theta(z)$is vanishing on the boundaries because the boundary layers are isothermal. From this figure we can observe that for small values of c, $\Theta(z)$is symmetric about the midpoint of the fluid layer. As c increases the temperature perturbation becomes confined to a small region near the bottom of the fluid layer where the fluid is less viscous.

Figures 12 and 13, show the effect of salinity Rayleigh number$(R_s)$for different values of viscosity variation c and largeP_r.The straight lines which represent the variation of the critical Rayleigh number with the salinity Rayleigh number are the lines with positive slopes. The temperature dependent viscosity variation (i.e., the values for $c \neq 0$) displaces the straight line downwards. The lowering of the critical Rayleigh numbers clearly shows that the system destabilizes with increasing viscosity ratio c and salinity gradient (R_s).We can also observe that as permeability K decreases the destabilizing effect of variable viscosity on the critical Rayleigh number is large.

Figures 14 and 15, show the occurrence of stationary convection and oscillatory convection for the given values of physical parameters. Figures 5.14 and 5.15, are plotted for $c = 0$ and $c = 5$respectively. In these figures green lines correspond to stationary convection and red lines correspond to oscillatory convection. Green lines are plotted for $R_{sc}$and red lines are plotted for $R_{0c}$for different values of R_s.The intersection point of green line and red line is given by $R_s = R_s^*$.For the values $R_s < R_s^*$,we get only stationary convection at the onset. For the values $R_s > R_s^*$,we get always get oscillatory convection at the onset. The values on the green lines gives pitchfork bifurcation and the values on the dotted lines give Hopf bifurcation. These two bifurcations are known as primary bifurcations (co-dimension one bifurcations). At $R_s = R_s^*$,we get co-dimension two-bifurcation point,

©2016, IJERMT All Rights Reserved

where$R_{sc} = R_{0c}$and $q_{sc} \neq q_{0c}$.It is noticed that Figures 14 and 15, are plotted for finite Prandtl numbers. We can also observe that as c and $D_a$increases co-dimension two bifurcation point decreases.

The behavior of $W(z)$and $\Theta(z)$of oscillatory convection near the onset is similar to the behavior of $W(z)$and $\Theta(z)$of stationary convection. Due to this reason we have omitted the numerical results related to $W(z)$and $\Theta(z)$of oscillatory convection.

V. CONCLUSIONS

The thermohaline convection with temperature dependent variable viscosity in a sparsely packed porous media has been studied by using linear stability analysis for$R/R, R/F, F/R,$ and F/Fboundary conditions. The onset of convection is studied by considering Darcy-Brinkman-Lapwood model. The presence of sparely packed porous media strongly effects the onset of convection. Due to double diffusive mechanism we may get stationary convection or oscillatory convection at the onset. It is noticed that the type of convection (stationaryconvection/oscillatory convection) depends on the physical parameters but not on the type of the boundary conditions. Based on the numerical results the range of viscosity ratio is divided three parts, namely, low viscosity ratio region, moderate viscosity ratio region, large viscosity ratio region. The results shows that for large Prandtl number obtained only stationary convection at the onset exist. Oscillatory convection is obtained for finite values of P_r.Some of the main results are listed below:

- In moderate and large viscosity ratio region, as c increases R_{sc} decreases,i.e., increasing c values destabilizes the onset stationary convection.
- As the physical parameter $R_s(>0)$ increases $R_{sc}$and R_{0c}also increases.This result shows that the increasing values of Rs stabilizes the onset ofstationary and oscillatory convection.
- As the Lewis number L increases $R_{sc}$and R_{0c}decreases. Which indicatesthat the effect of L destabilizes the onset of convection.
- As $P_r$increases R_{0c}decreases. This result implies that increasing values $P_r$destabilizes the onset of oscillatory convection.
- The above said behaviors of $R_{sc}$and R_{0c}in the low and moderate viscosityratio regions is quiet opposite, in the absence of porous media.
- The maximum value of z component of vertical velocity $W(z)$on the curve increases as c increases. The maximum value of $W(z)$occurs at the bottom warm boundary where the fluid is less viscous for a given c.
- The maximum value of z component of temperature $\Theta(z)$on the curvedecreases as c increases. The maximum value of $\Theta(z)$occurs at the bottomwarm boundary where the fluid is less viscous for a given c. This showsthat temperature perturbations confined to low viscosity region.
- For large P_r as D_a increases R_{sc} decreases. This shows that the effect ofDastabilizes the onset of stationary convection.
- The occurrence of stationary convection or oscillatory convection at theonset also depends on $R_s > 0$ for finiteP_r.The occurrence of co-dimensiontwo bifurcation point is also observed.

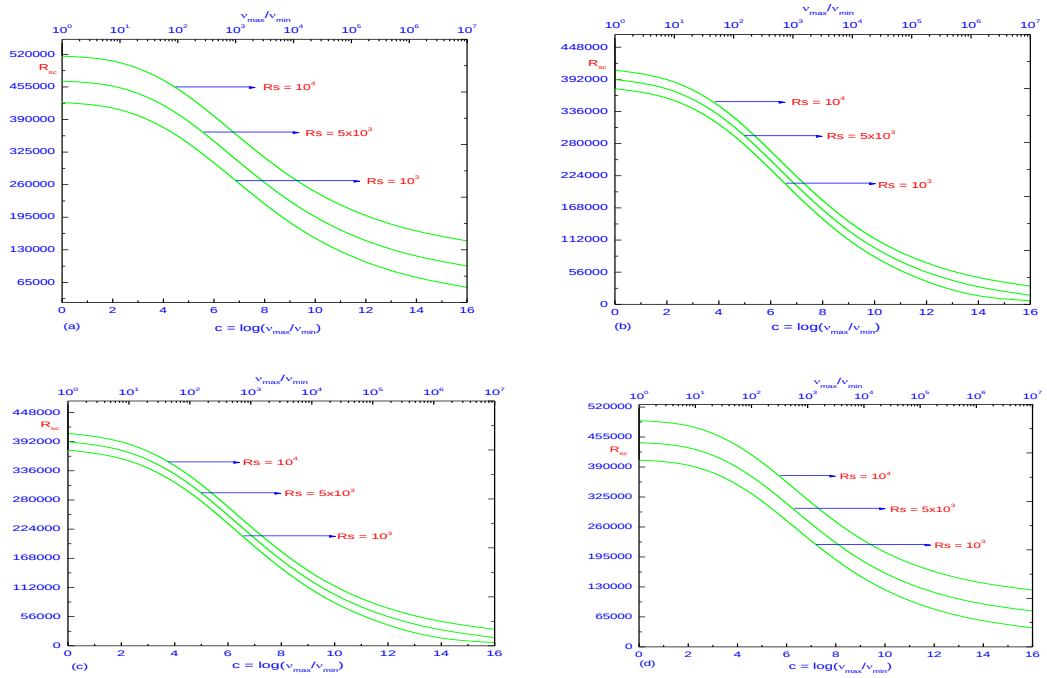

Figure 2:The effect of salinity Rayleigh number R_s and viscosity ratio c on critical Rayleigh number R_{sc}. Numerically plotted neutral stability curves to represent the onset of stationary convection for exponential fluid. Figs. 5.1(a-d) are plotted for R/R, R/F, F/R, and F/F boundary conditions respectively (for Lewis number $L = 0.1$and Darcy number $D_a = 10^{-4}$and large P_r.

©2016, IJERMT All Rights Reserved

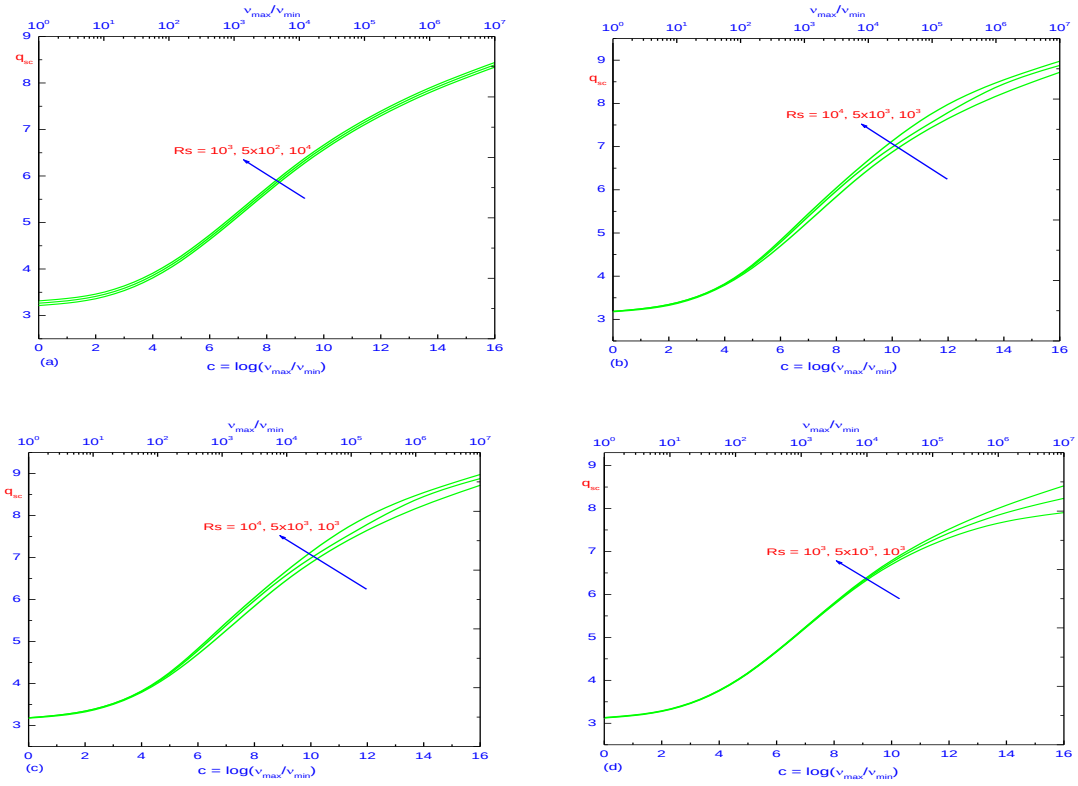

Figure 3:The effect of salinity Rayleigh number R_s and viscosity ratio c on critical Rayleigh number q_{sc}. Numerically plotted neutral stability curves to represent the onset of stationary convection for exponential fluid. Figs. 5.1(a-d) are plotted for R/R, R/F, F/R, and F/F boundary conditions respectively (for Lewis number $L = 0.1$and Darcy number $D_a = 10^{-4}$and large P_r).

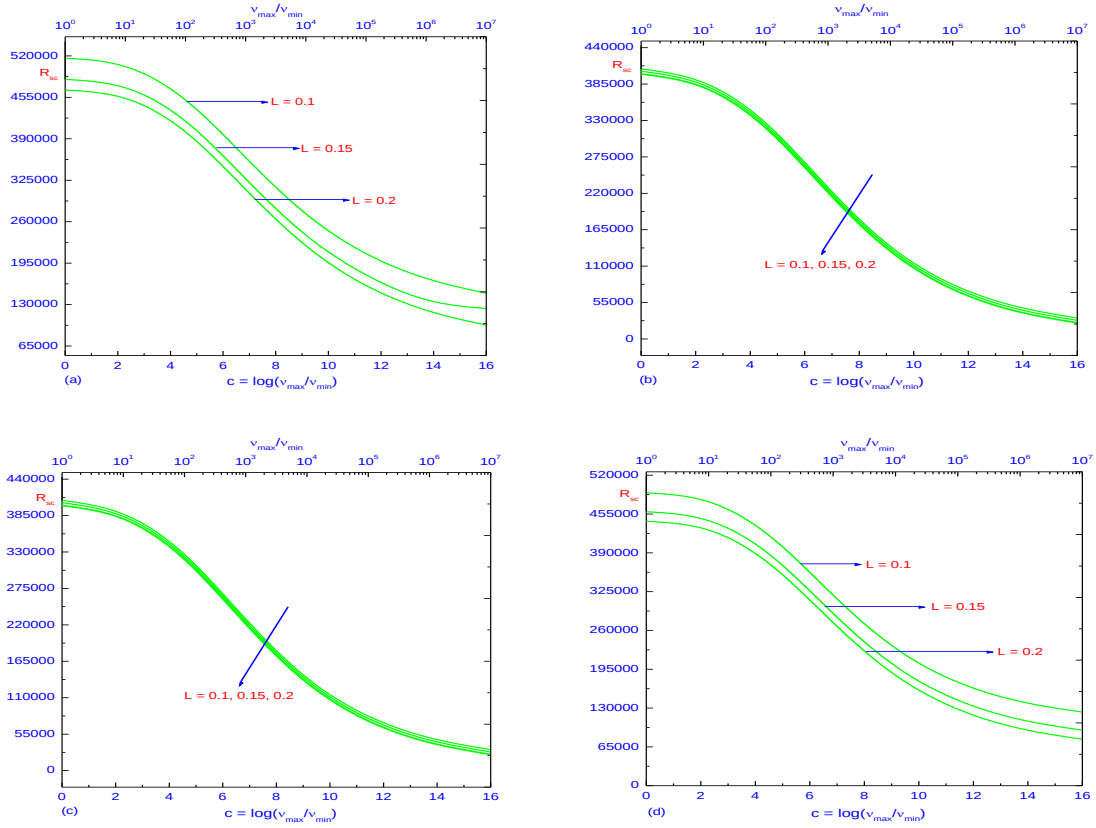

Figure 4: The effect of Lewis number L and viscosity ratio c on critical Rayleigh numberR_{sc}.Numerically plotted neutral stability curves to represent the onset of stationary convection for exponential fluid. Figs. 5.3(a-d) are plotted for R/R, R/F, F/R, and F/Fboundary conditions respectively (for salinity Rayleigh number $R_s = 10^4$and Darcy number $D_a = 10^{-4}$and large P_r).

©2016, IJERMT All Rights Reserved

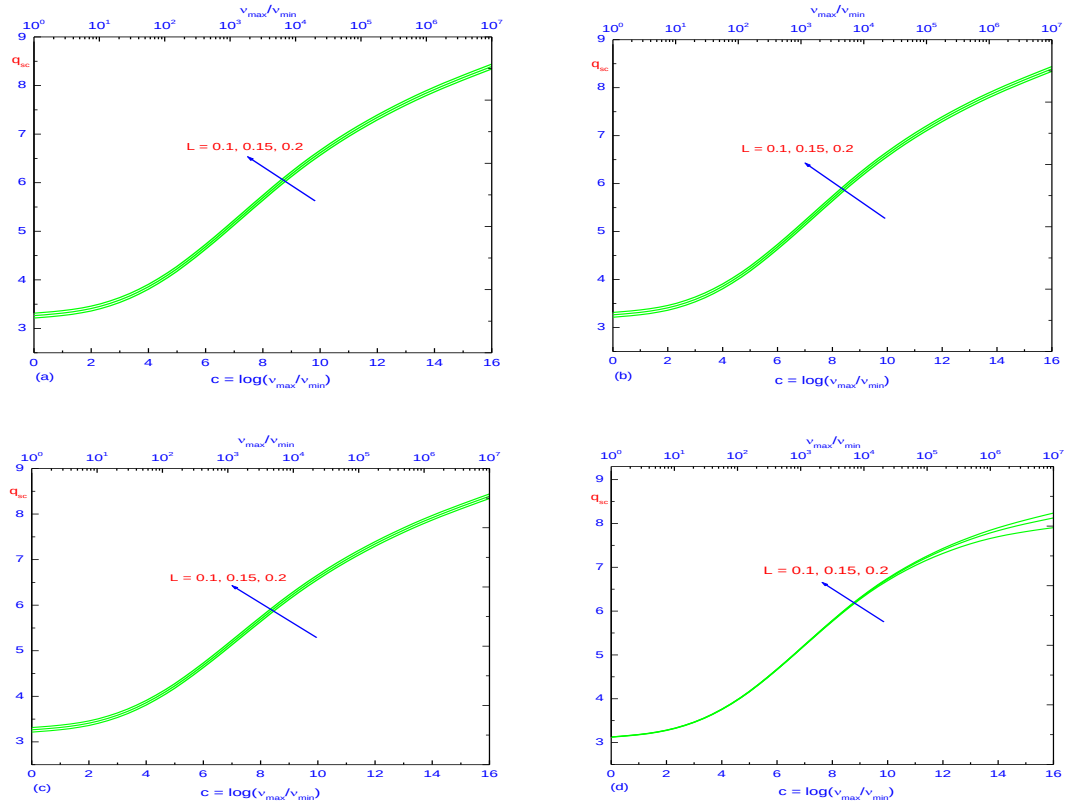

Figure 5: The effect of Lewis number L and viscosity ratio c on critical wave number q_{sc}.Numerically plotted neutral stability curves to represent the onset of stationary convection for exponential fluid. Figs. 5.4(a-d) are plotted for $R/R, R/F, F/R$, and F/F boundary conditions respectively (for salinity Rayleigh number $R_s = 10^4$and Darcy number $D_a = 10^{-4}$and large P_r).

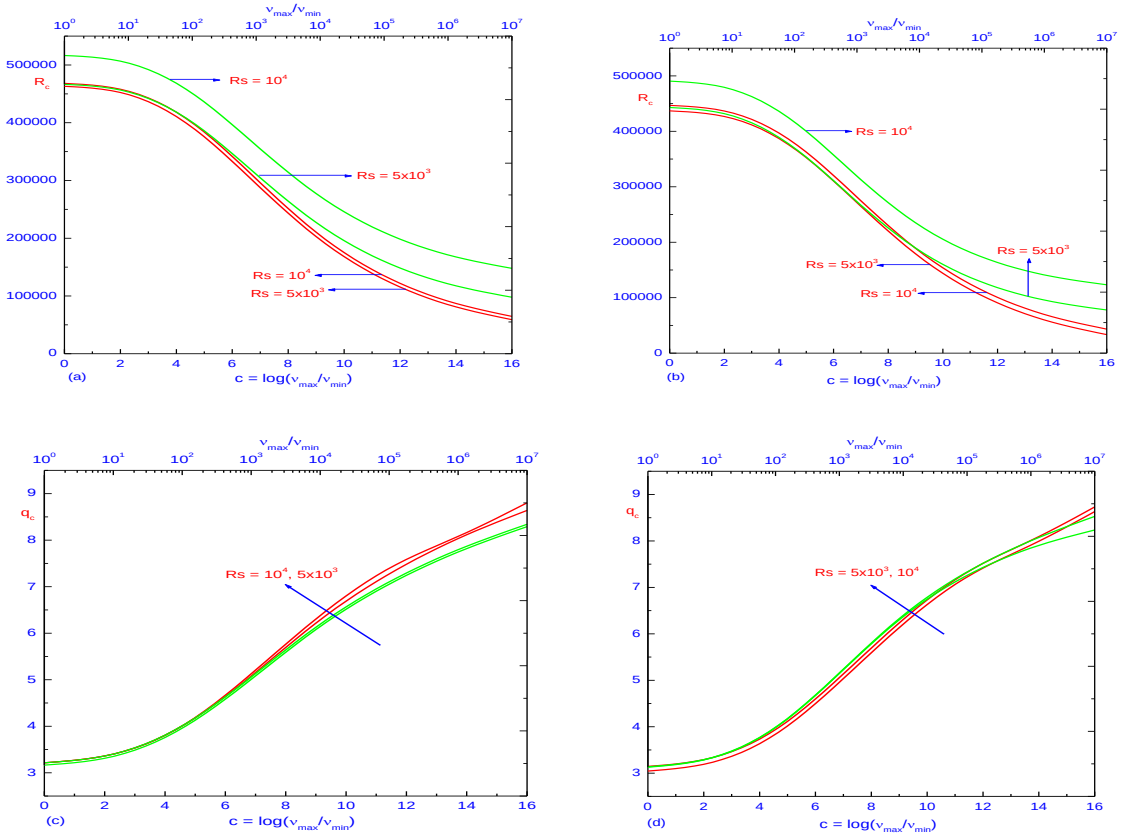

Figure 6: Critical Rayleigh number $R_c$and critical wave number $q_c$versus, viscosity ratio c, for $L = 0.1$, $D_a = 10^{-4}$ $\phi = 0.8$and $(P_r = 10^3)$. Figures (a) and (c) are plotted for R/R boundaries. Figures (b) and (d) are plotted for F/F boundaries. Green lines correspond to stationary convection. Red lines correspond to oscillatory convection.

©2016, IJERMT All Rights Reserved

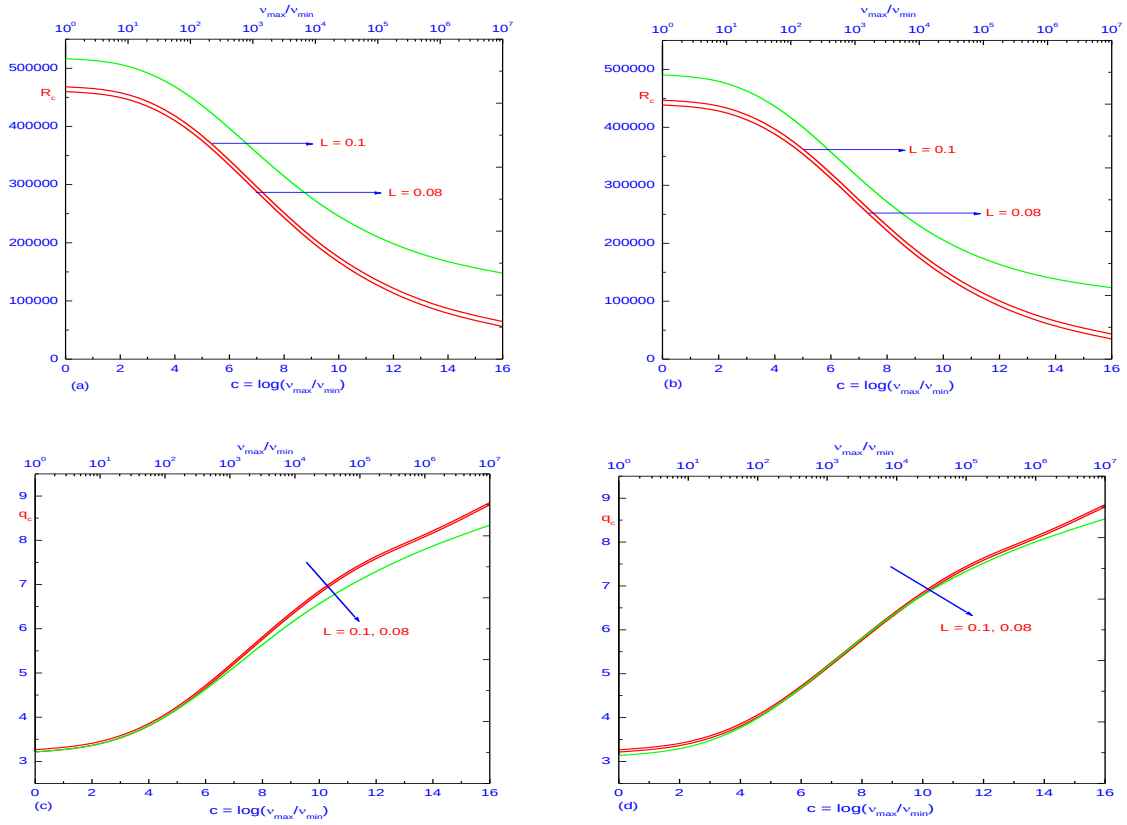

Figure 7: Critical Rayleigh number R_c and critical wave number q_c versus, viscosity ratio c, for $R_s = 10^4$, $D_a = 10^4$ $\phi = 0.8$and $(P_r = 10^3)$. Figures (a) and (c) are plotted for R/Rboundaries. Figures (b) and (d) are plotted for F/F boundaries. Green lines correspond to stationary convection. Red lines correspond to oscillatory convection.

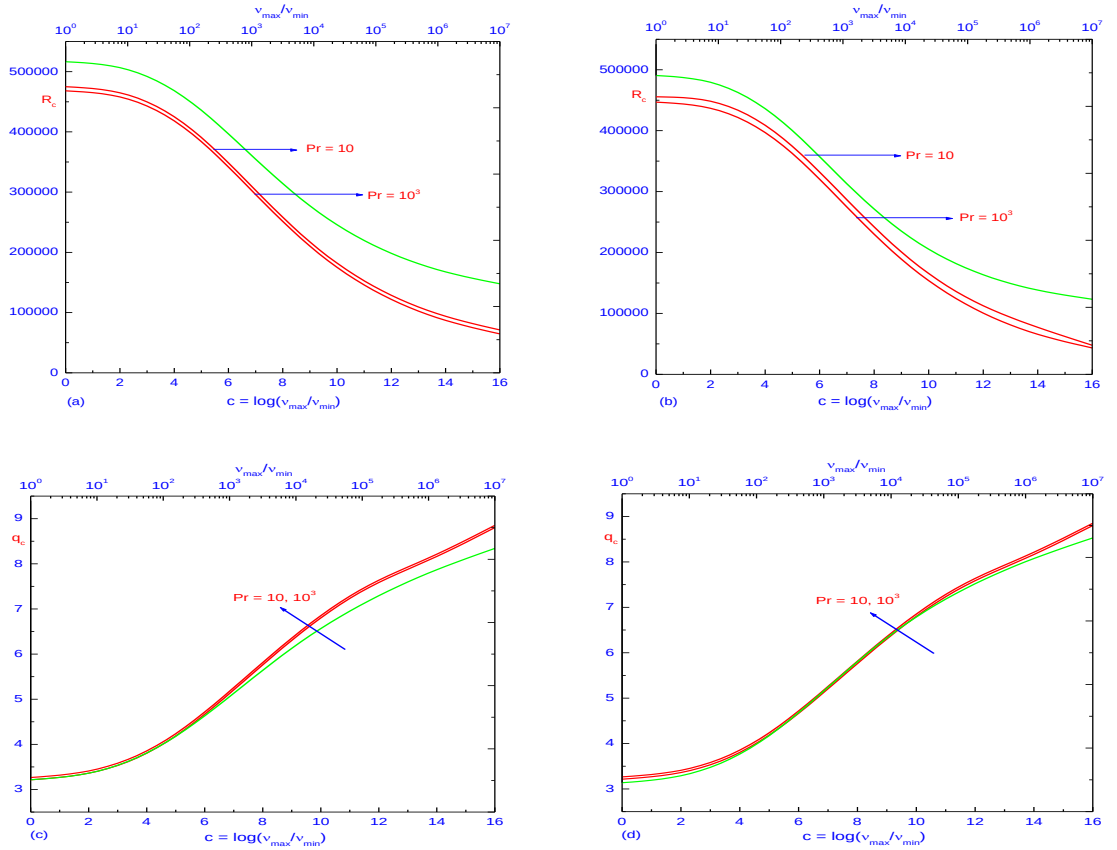

Figure 8: Critical Rayleigh number R_c and critical wave number q_c versus, viscosity ratio c, for $L = 0.1$, $R_s = 10^4$, $D_a = 10^{-4}$and$\phi = 0.8$Figures (a) and (c) are plotted for R/R boundaries. Figures (b) and (d) are plotted for F/ Fboundaries. Green lines correspond to stationary convection. Red lines correspond to oscillatory convection.

©2016, IJERMT All Rights Reserved

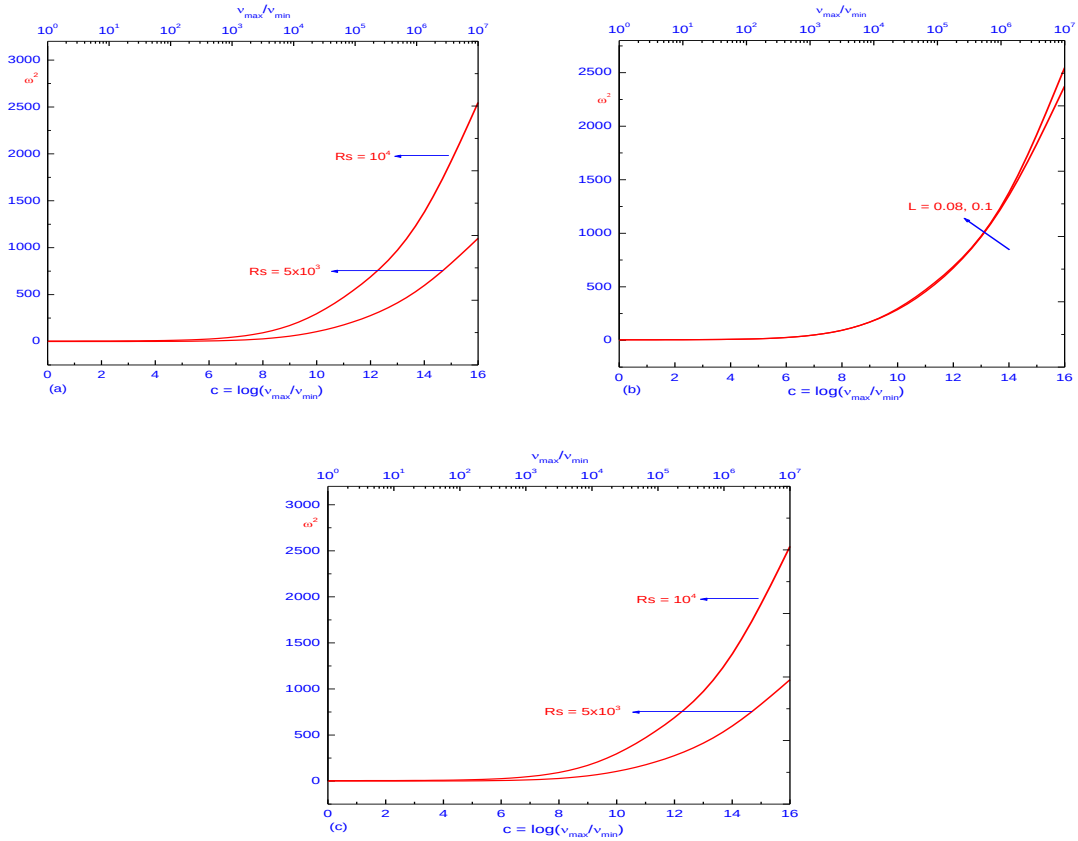

Figure 9: The effect of viscosity variation c on w^2 for different physical parameters with $D_a = 10^{-4}$ and $\phi = 0.8$. Fig. (a) is plotted for $P_r = 10^3, L = 0.1$, Fig. (b) is plotted for $P_r = 10^3$, $R_s = 10^4$ and Fig. (c) is plotted for $L = 0.1$, $R_s = 10^4$, Above figures are plotted for R/R boundary conditions.

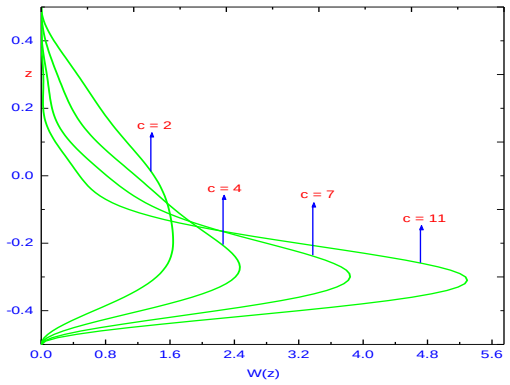

Figure 10: The vertical velocity eigenfunctions W(z) are plotted for different c values and R/R boundary conditions with $L = 0.1$, $R_s = 10^4, D_a = 10^{-4}$, $\phi = 0.8$ and large P_r.

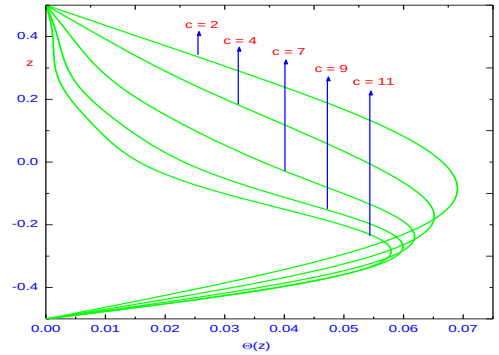

Figure 11: Temperature perturbation Θ(z) for different values of viscosity ratio c with $L = 0.1$, $R_s = 10^4$, $D_a = 10^{-4}$ and $\phi = 0.8$, and large P_r for R/R boundary conditions.

©2016, IJERMT All Rights Reserved

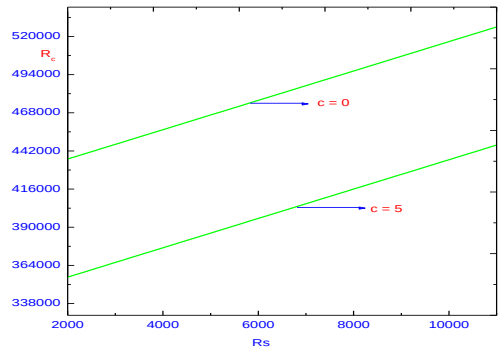

Figure 12: Effect of salinity Rayleigh number and viscosity variation c on critical Rayleigh number with$L = 0.1$, $R_s = 10^4$, $\phi = 0.8$ and $D_a = 10^{-4}$ and large P_r for stationary convection. This figure is plotted for R/R boundary conditions.

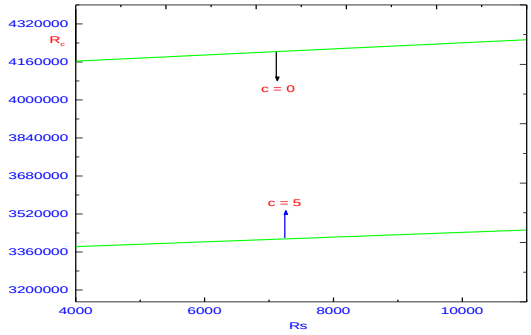

Figure 13: Effect of salinity Rayleigh number and viscosity variation c on critical Rayleigh number with $L = 0.1$, $R_s = 10^4$, $\phi = 0.8$ and $D_a = 10^{-5}$ and large P_r for stationary convection. This figure is plotted for R/R boundary conditions.

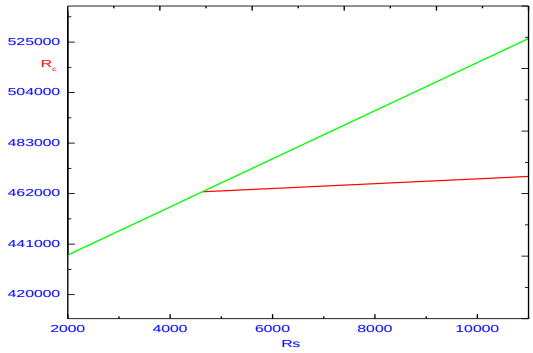

Figure 14: Effect of salinity Rayleigh number and viscosity variation c on critical Rayleigh number with $L = 0.1$, $R_s = 10^4$,$D_a = 10^{-4}$ and $\phi = 0.8$ for stationary convection (green lines) and $P_r = 10^3$for oscillatory convection (red lines). This figure is plotted for R/Rboundary conditions.

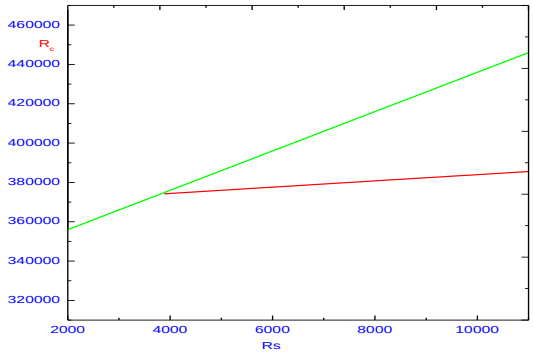

Figure 15: Effect of salinity Rayleigh number and viscosity variation c on critical Rayleigh number with $L = 0.1$, $R_s = 10^4$and $D_a = 10^{-5}$ and $\phi = 0.8$for stationary convection (green lines) and $P_r = 10^3$ for oscillatory convection(red lines). This figure is plotted for R/R boundary conditions.

©2016, IJERMT All Rights Reserved

REFERENCES

[1] R.J.M. De West, *Flow through porous media,* Academic Press, New York, 1965.
[2] M. Harr, *Ground water and Seepage,* McGraw-Hill, New-York, 1962.
[3] C.M. Marle,*Multiphase Flow in Porous Media,* Gulf Publishing Houston, TX, 1981.
[4] M. Muskat, *Flow of Homogeneous fluid through porous media,*McGraw-Hill, New York, 1937.
[5] R.A. Greenkorn, *Steady flow through porous media,* AICHE J.27: (1981), pp.527.
[6] N.Rudraiah, B.C. Chandrasekhar, R. Veerabhadraiah, and S.T. Nagaraj, *Some flow problems in porous media,* PGSAM-2, Bangalore University, India, (1979).
[7] N.Rudraiah, *Flow past porous layers and their stability,*and Encyclopedia of Fluid Mechanics, Slurry Flow Technology, Gulf Publishing, Chap., 14(1986), pp.567.
[8] N.Rudraiah, *Transfer in Composite Material,* Sectional Presidential Address at the 76th Science Congress, Indian Science Congress Association, Calcutta, India (1988).
[9] D.A. Neild,*The limitations of the Brinkman-Forchheimer equation in modeling flow in a saturated porous medium and at an interface,* Int. J. Heat Fluid Flow, 12 (3) (1991), pp. 269.
[10] A. Bejan and D. Poulikakos, *The non-Darcy regime for vertical boundary layer natural convection in a porous medium,* Int. J. Haet and Mass Transfer, 27 (1984), pp. 717.
[11] M. Keviani, Gradient*destruction in flow through a rigid matrix,* J. Fluid Mech., 165 (1986), pp. 221.
[12] G. Neale and W. Nader, *Practical significance of Brinkman's extension to Darcy's law*: *Coupled paralleled flows within a channel and a bounding porous medium,* Cand. J. Chem. Eng., 52 (1974), pp. 475.
[13] Y.C. Fung and H.T.Tang, *Fluid movement in a channel with permeable walls covered by porous media,* J.Appl. Mech., 97(1975), pp. 45.
[14] F. W.Wiegel, *Fluid flow through porous macromolecular systems in Lecture Notes in physics,* Spriger-Verlag, NewYork, (1980).
[15] F.W.Wiegel, and P.F.Mijnlieff, *Comments on the Debje-Brinkman equation,* Physica A, 85(1976), pp. 207.
[16] S.Whitaker, *Simultaneous heat, mass and momentum transfer in porous media: A theory of drying, Adv.Heat Transfer* (1977), pp. 119.
[17] G.S.Breavers and E.Sparrow, *Non-Darcian flow through fibrous porous media,* J.Appl.Mech., 36(1969), pp. 711.
[18] J.F.Brady, *Flow development in a porous channel and tube,* Phys. Fluids, 27(1984), pp. 1061.
[19] B.C. Chandrasekhara and D.Vortmayer, *Flow models for velocity distribution in fixed porous beds under isothermal condition,* Thermo Fluid Dynamics, 12(1979), pp. 105.
[20] S.M. Hussanizadeh and W.G.Gray, *High velocity flow in porous media,* Transport Porous Media, 2(1987), pp. 521.
[21] N.Rudraiah and Rao S.Balachandran, *Study of nonlinear convection in a sparsely packed porous medium using spectral analysis,* Appl. Sci.Res., 40(3)(1983), pp. 223.
[22] G.Veronis, *Effect of a stabilizing gradient of solute on thermal convection,* J.Fluid Mech., 34(1968), pp. 315.
[23] H. Rubin, *Effect of nonlinear stabilizing salinity profiles on thermal convection in a porous medium layer.* Water Resour. Res., 9(1973), pp. 211.
[24] H. Rubin, *Effect of solute dispersion on thermal convection in a porous medium layer.* Water Resour. Res., 9(1973), pp. 968.
[25] D.A. Neild, *Onset of thermohaline convection in porous medium.* Water Resour. Res., 4(1968), pp. 553.
[26] N.Rudraiah, I.S.Shivakumara and R.Fredcich, *The effect of rotation on linear and non-linear double-diffusive convection in a sparcely packed porous medium,* Int. J. Heat and Mass Tran., 29(9)(1986), pp. 1301.
[27] K.C.Stengel, D.S.Oliver, and J.R.Booker, *Onset of convection in a variable viscosity fluid,* J. Fluid Mech., 120(1982), pp. 411.
[28] K.E. Torrence and D.L. Turcotte, *Thermal convection with large viscosity variation,* J. Fluid Mech., 47(1971), pp. 113.
[29] KG. Stengel, *Onset of convection in a variable viscosity fluid,* M. S. Thesis, University of Washington.

©2016, IJERMT All Rights Reserved